MicroRNA-126 protects SH-SY5Y cells from ischemia/reperfusion injury-induced apoptosis by inhibiting RAB3IP

ZHUMEI SUN[1*], XU ZHAO[2*], MEIHANG ZHANG[1], NING LI[2], YANNING ZHAO[3], CHANGXIANG CHEN[3], JIANMIN LI[1], YANJUAN GUO[2] and QIANG FENG[4]

[1]Department of Clinical Medicine, North China University of Science and Technology, Tangshan, Hubei 063210; [2]Department of Neurosurgery, Affiliated Hospital of North China University of Science and Technology, Tangshan, Hubei 063000; [3]Department of Nursing and Rehabilitation, North China University of Science and Technology, Tangshan, Hubei 063210; [4]Department of Cardiology, Handan Central Hospital, Handan, Hubei 056001, P.R. China

Received June 9, 2021; Accepted September 29, 2021

DOI: 10.3892/mmr.2021.12578

Abstract. MicroRNA (miR)-126 is known to inhibit inflammatory responses in various inflammatory-related diseases, but its role during the cerebral ischemia/reperfusion (I/R) injury remains unknown. The present study aimed to examine the interaction between miR-126 and RAB3A interacting protein (RAB3IP), and explore its potential protective effects during I/R injury. The human neuroblastoma cell line SH-SY5Y was cultured in an oxygen-glucose deprivation/reoxygenation (OGD/R) environment to simulate I/R injury to assess miR-126 expression and cell viability. SH-SY5Y cells cultured in normal conditions were used as a negative control (NC) group. SH-SY5Y cells were transfected with a miR-126 mimic or an NC mimic, then cultured in OGD/R conditions; in rescue experiments, SH-SY5Y cells were co-transfected with RAB3IP overexpression or NC plasmid together with mimic-NC or mimic-miR, and then maintained in an OGD/R environment to evaluate miR-126, RAB3IP expression, cell viability and apoptosis. Cell viability was reduced in the Model group compared with the NC group, suggesting the successful construction of the OGD/R model. miR-126 expression was downregulated in the Model group compared with the NC group. However, following transfection with mimic-miR, cell viability increased compared with the mimic-NC group. Annexin V and PI staining and Hoechst/PI assays also indicated that apoptosis was reduced in the mimic-miR group compared with the mimic-NC group. RAB3IP expression was reduced following mimic-miR transfection. In rescue experiments, miR-126 negatively regulated RAB3IP expression; by contrast, RAB3IP did not affect that of miR-126. In addition, RAB3IP overexpression attenuated the protective effect of miR-126 on OGD/R-induced apoptosis. These findings suggest that miR-126 protects against cerebral I/R injury by targeting RAB3IP.

Correspondence to: Dr Zhumei Sun, Department of Clinical Medicine, North China University of Science and Technology, 57 Jianshe South Road, Lubei, Tangshan, Hubei 063210, P.R. China
E-mail: zhujichuo1870@163.com

Dr Xu Zhao, Department of Neurosurgery, Affiliated Hospital of North China University of Science and Technology, 73 Jianshe South Road, Lubei, Tangshan, Hubei 063000, P.R. China
E-mail: xufei1488@163.com

[*]Contributed equally

Key words: microRNA-126, Ras-related protein RAB3A interacting protein, oxygen-glucose deprivation/reoxygenation model, cerebral ischemia/reperfusion injury, cell viability, apoptosis

Introduction

Ischemic brain injury is a serious neurological condition and the third most common cause of death worldwide (1-3). Immediate restoration of blood flow is recommended as the standard treatment for brain ischemia, which not only delivers oxygen and transports nutrients to sustain aerobic metabolism and ATP generation, but also eliminates accumulated H^+ ions to normalize extracellular pH (4-7). However, ischemia/reperfusion (I/R) may exacerbate the risk of brain tissue injury (8). Due, in part, to overconsumption of oxygen, intracellular Ca^{2+} overload or redistribution during the first minutes of reperfusion, cerebral I/R contributes to the destruction of the mitochondrial respiratory chain response, excessive production of pro-inflammatory mediators in the damaged areas of the brain tissue, as well as massive deposition of Ca^{2+} ions in the pericytes, which further increases the damage to neurons (5). Despite significant improvements in timely reperfusion strategies (such as advanced surgical equipment, as well as safe and effective antiplatelet and antithrombotic agents), effective therapy for the prevention of cerebral I/R injury is still lacking (9,10). Therefore, it is essential to examine the underlying mechanism of cerebral I/R injury, as this may help the development of prevention strategies for cerebral I/R injury.

Several microRNA (miRNA/miR) molecules are considered important regulators of neuronal survival during cerebral I/R injury (11-15). miR-126 is a family of extensively studied miRNA molecules known to inhibit inflammatory responses in

various inflammatory-related diseases (16,17). In a Parkinson's disease model, miR-126 markedly increased neuronal cell proliferation and reduced apoptosis by targeting Ras-related protein RAB3A interacting protein (RAB3IP) (18). Moreover, this miRNA also interacts with various genes, including nuclear factor erythroid 2 like 2 (Nrf2), to attenuate I/R injury (19,20). Based on the aforementioned findings, it was hypothesized in the present study that miR-126 may play a protective role in cerebral I/R injury by targeting RAB3IP. Therefore, the aim of the present study was to establish an oxygen-glucose deprivation/reoxygenation (OGD/R) model to simulate cerebral I/R injury, in order to examine the interaction between miR-126 and RAB3IP and explore its potential protective effect during cerebral I/R injury.

Materials and methods

Cell culture. The human SH-SY5Y neuroblastoma cell line was purchased from the American Type Culture Collection (ATCC; cat. no. CRL-2266). The authenticity of the cells was confirmed using the Short Tandem Repeat assay report available at https://www.procell.com.cn/view/1401.html. The cell line was cultured according to the ATCC protocol. Briefly, cells were maintained in Eagle's Minimum Essential Medium (EMEM; cat. no. M4655; MilliporeSigma) supplemented with 10% FBS (cat. no. 12103C; MilliporeSigma) in a humidified incubator at 37˚C with 5% CO_2. The 293T cells were also purchased from the ATCC and maintained in DMEM (cat. no. D0819; MilliporeSigma) supplemented with 10% FBS in a humidified incubator at 37˚C with 5% CO_2. The 100 U/ml penicillin and 100 μg/ml streptomycin (cat. no. 10378016; Gibco; Thermo Fisher Scientific, Inc.) were added in EMEM and DMEM.

Establishment of the OGD/R model. In order to simulate cerebral I/R injury *in vitro*, an OGD/R model was established as described previously (21-24). Briefly, SH-SY5Y cells were seeded in plates pre-coated with poly-L-lysine (cat. no. P8920; MilliporeSigma) and incubated in glucose-free EMEM under hypoxic conditions (1% O_2; 5% CO_2; 94% N_2) at 37˚C for 4 h. The cells were then transferred to normal EMEM and maintained in normal conditions (5% CO_2; 95% air) at 37˚C for 48 h (Model group). SH-SY5Y cells continuously maintained in normal EMEM under normal incubation conditions were used as a negative control (NC group). All subsequent experiments were conducted in three replicates.

Transfection. miR-126 mimic (mimic-miR; 5'-CATTATTAC TTTTGGTACGCG-3') and mimic-NC (cat. no. B04001) were purchased from Shanghai GenePharma Co., Ltd. Lipofectamine® 3000 (cat. no. L3000075; Invitrogen; Thermo Fisher Scientific, Inc.) was used to transfect 0.5 pM mimic-miR and 0.5 pM mimic-NC into $1x10^6$ SH-SY5Y cells according to the manufacturer's instructions. The transfected cells (24 h after transfection) were then subjected to OGD/R treatment. Untransfected SH-SY5Y cells that underwent OGD/R treatment alone (Model group) were also used as a control. Each assay was only performed once, but with three wells.

Rescue experiments. RAB3IP overexpression plasmid (OE-RAB3IP) and the OE-NC plasmid (an empty vector) were generated using the pcDNA3.1 vector purchased from Shanghai GenePharma Co., Ltd. SH-SY5Y cells ($1x10^6$) were co-transfected with 0.8 μg OE-NC or 0.8 μg OE-RAB3IP vector, together with mimic-NC or mimic-miR using Lipofectamine® 3000 at 37˚C for 24 h. The transfected cells (24 h after transfection) were subjected to OGD/R treatment. Thus, the experiment involved the following four groups: i) OE-NC + mimic-NC; ii) OE-RAB3IP + mimic-NC; iii) OE-NC + mimic-miR; and iv) OE-RAB3IP + mimic-miR. Each assay was only performed once, but with three wells.

Reverse transcription-quantitative PCR (RT-qPCR). Total RNA of cells was extracted using TRIzol® (Invitrogen; Thermo Fisher Scientific, Inc.), then reverse transcribed into cDNA using the ReverTra Ace® qPCR RT kit (cat. no. FSQ-101; Toyobo Life Science) according to the kit's instruction. qPCR was carried out using SYBR® Green Realtime PCR Master Mix (cat. no. QPK-20; Toyobo Life Science). The thermocycling conditions included an initial denaturation at 95˚C for 5 min, followed by 40 cycles of 95˚C for 5 sec and 61˚C for 30 sec. The primers sequences are presented in Table I. The expression levels of miR-126 and RAB3IP were calculated using the $2^{-\Delta\Delta Cq}$ method (25). GAPDH (for mRNA) and U6 (for miRNA) served as internal references. Besides, the forward and reverse primers of miR-126 were designed according to previous studies (26,27). Each assay was only performed once, but with three wells.

Western blot assay. Total protein of cells was extracted using RIPA lysis buffer (cat. no. R0278; MilliporeSigma). The BCA Assay Kit for Protein Determination (cat. no. BCA1; MilliporeSigma) was used to measure the protein concentration. Subsequently, the protein samples (20 μg) were separated via 4-20% SDS-PAGE and subsequently transferred to PVDF membranes (cat. no. IPVH00010; MilliporeSigma). The membranes were then blocked with 5% skimmed milk for 2 h at 37˚C and incubated with the primary antibodies (Table II) overnight at 4˚C. Following the primary antibody incubation, the membranes were incubated with secondary antibodies (Table II) for 1.5 h at room temperature. The visualization of the protein bands was performed using Pierce™ ECL Plus Western Blotting Substrate (cat. no. 32132X3; Thermo Fisher Scientific, Inc.) with exposure on X-ray film (cat. no. 1753185; Kodak). GAPDH was used as the internal reference. Each assay was only performed once, but with three wells. The protein bands were analyzed using ImageJ 1.8.0 software (National Institutes of Health).

Cell Counting Kit-8 (CCK-8) assay. A volume of 10 μl CCK-8 solution (cat. no. CK04; Dojindo Laboratories, Inc.) and 90 μl RPMI-1640 medium were added to the cells in each plate, which were then incubated at 37˚C with 5% CO_2 for 2 h. The absorbance was measured using a microplate reader. Each assay was only performed once, but with three wells.

Cell cycle assay. The Cell Cycle Assay kit (cat. no. C543; Dojindo Laboratories, Inc.) was used to analyze cell cycle progression. The cells were harvested, counted and re-suspended in PBS (cat. no. 806552; MilliporeSigma), then fixed with 70% ethanol (cat. no. A500737; Sangon Biotech

Table I. Primer sequences.

Gene	Forward primer (5'→3')	Reverse primer (5'→3')
miR-126	ACACTCCAGCTGGGCATTATTACTTTTGGT	TGTCGTGGAGTCGGCAATTC
RAB3IP	GTGTCATCTACCGGCCACAC	CCCTCTGAGCTTTTGCGAGT
U6	CGCTTCGGCAGCACATATACTA	ATGGAACGCTTCACGAATTTGC
GAPDH	GACCACAGTCCATGCCATCAC	ACGCCTGCTTCACCACCTT

miR, microRNA; RAB3IP, Ras-related protein RAB3A interacting protein.

Table II. Antibodies used in western blotting.

A, Primary antibody

Antibody	Supplier	Cat. no.	Dilution
Rabbit polyclonal against RAB3IP	Invitrogen; Thermo Fisher Scientific, Inc.	PA5-96927	1:500
Rabbit monoclonal against GAPDH	Abcam	ab181602	1:5,000

B, Secondary antibody

Antibody	Supplier	Cat. no.	Dilution
HRP-labeled goat anti-rabbit IgG (H+L)	Abcam	ab6721	1:10,000

RAB3IP, Ras-related protein RAB3A interacting protein.

Co., Ltd.) at 4°C overnight. After discarding the ethanol, the cells were stained with working solution at 4°C for 1 h in the dark. The cells were then analyzed using a FACSCalibur flow cytometer (BD Biosciences). The data were analyzed using FlowJo 7.6 software (BD Biosciences). Each assay was only performed once, but with three wells.

Lactate dehydrogenase activity (LDH) assay. The LDH assay was performed using the LDH Assay Kit-WST (cat. no. CK12; Dojindo Laboratories, Inc.). A volume of 100 μl working solution was added and incubated with the cells in the dark for 20 min. Subsequently, 50 μl working solution was added. The absorbance was then measured using a microplate reader at 490 nm. Each assay was only performed once, but with three wells.

Annexin V (AV)/propidium iodide (PI) assay. Apoptosis was evaluated using an AV-FITC Apoptosis Detection kit (cat. no. 4830-01-K; R&D Systems, Inc.). The cells were resuspended in 100 μl binding buffer, then incubated with 5 μl AV and 5 μl PI for 15 min at room temperature in the dark. Apoptotic cells were analyzed using a FACSCalibur flow cytometer (BD Biosciences). The data were analyzed with FlowJo 7.6 software (BD Biosciences), and the percent of late or early + late apoptosis cells was assessed. Each assay was only performed once, but with three wells.

Hoechst/PI assay. Hoechst/PI assay was performed to assess cell apoptosis. The culture medium was discarded, and PBS was added to the wells. Subsequently, 1 μl Hoechst 33342 (cat. no. B2261; MilliporeSigma) and 1 μl PI (cat. no. P4864; MilliporeSigma) were added to each well and incubated at 4°C for 20 min. An inverted fluorescence microscope (Olympus Corporation) was used to determine the percentage of apoptotic cells. Each assay was only performed once, but with three wells.

Luciferase activity assay. The fragments of the RAB3IP 3' untranslated region (UTR) containing the wild-type (WT) miR-126 binding sites (RAB3IP-WT) or mutant (MT) binding sites (RAB3IP-MT; synthesized by Sangon Biotech Co., Ltd.) were cloned into the pmirGLO vector (cat. no. E1330; Promega Corporation). The 293T cells were seeded in 24-well plates ($5x10^4$ cells/well) and cultured to 80% confluence. Subsequently, 100 ng RAB3IP-WT or RAB3IP-MT luciferase vector and 50 nM mimic-miR or mimic-NC were co-transfected into 293T cells for 48 h using Lipofectamine 3000. The Dual-Luciferase Reporter Assay system (cat. no. E1910; Promega Corporation) was used to measure relative luciferase reporter activity. Luciferase activity was normalized to *Renilla* luciferase activity. Each assay was only performed once, but with three wells.

Statistical analysis. SPSS 26.0 (IBM Corp.) was used for data analysis. The data are presented as the mean ± standard deviation. Comparisons between two groups were carried out using an unpaired Student's t-test. Multi-group comparisons were performed using a one-way ANOVA followed by a Tukey's

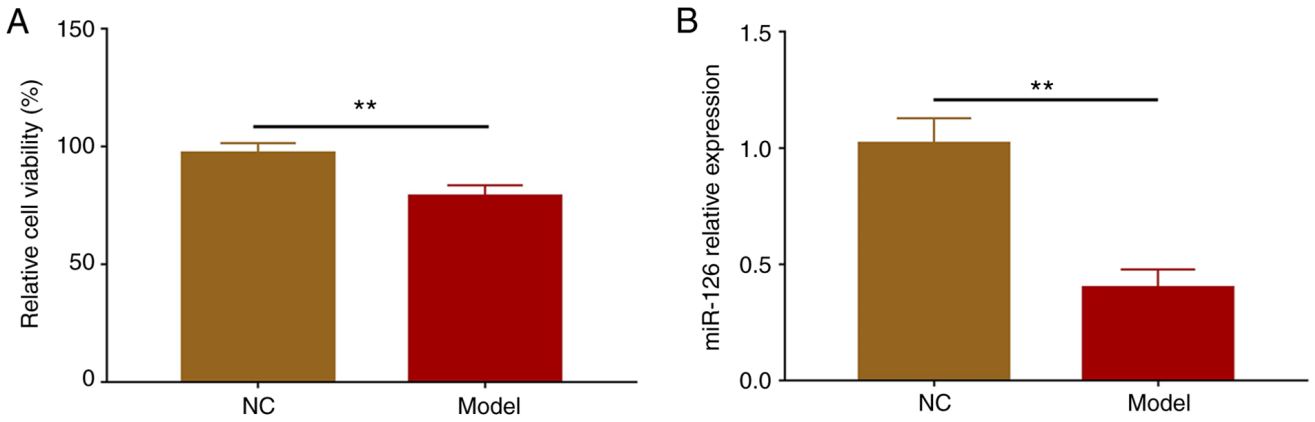

Figure 1. Successful establishment of the oxygen-glucose deprivation/reoxygenation model, demonstrating increased miR-126 expression. (A) Relative cell viability and (B) miR-126 expression levels were determined using Cell Counting Kit-8 assays and reverse transcription-quantitative PCR, respectively. n=3. The data were analyzed using unpaired Student's t-tests. **P<0.01. NC, negative control; miR-126, microRNA-126.

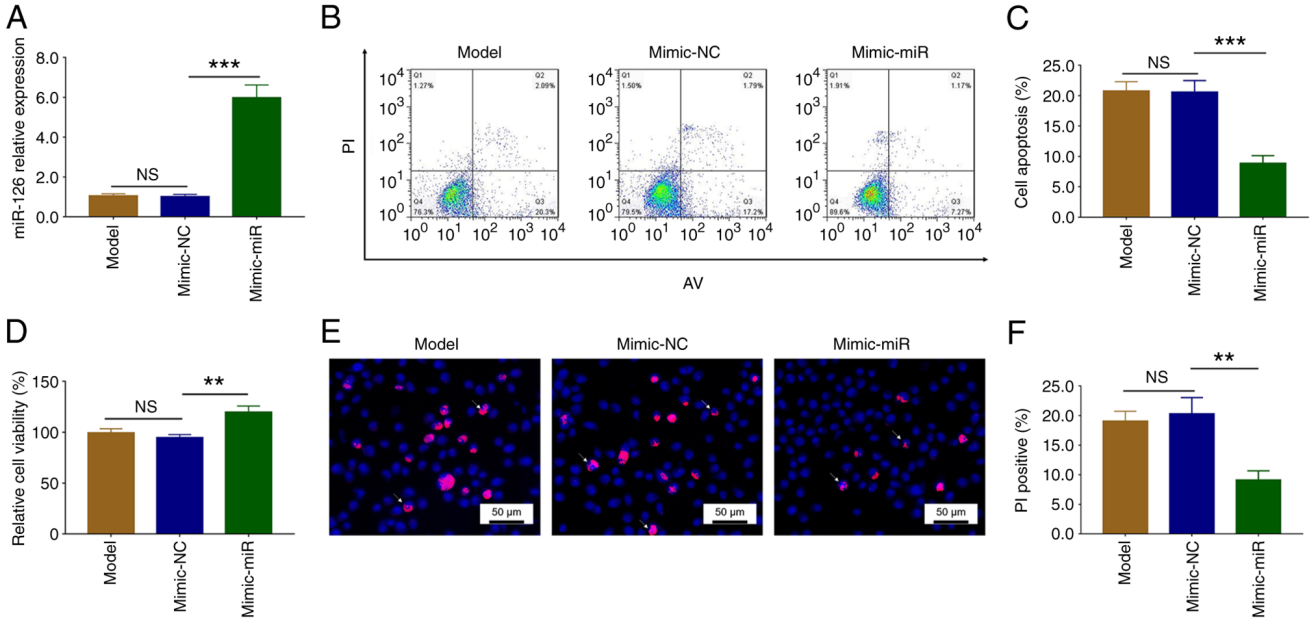

Figure 2. Effect of miR-126 on cell viability and apoptosis during cerebral ischemia/reperfusion injury. (A) miR-126 expression levels were determined using reverse transcription-quantitative PCR. (B and C) Apoptosis was examined using AV/PI staining. (D) Cell viability was determined using Cell Counting Kit-8 assays. (E and F) Apoptosis was examined using Hoechst/PI staining. The mimic-NC was used as the NC for mimic-miR transfection. Untransfected cells subjected to oxygen-glucose deprivation/reoxygenation were also used as an additional control (Model group). n=3. The data were analyzed using one-way ANOVA followed by Tukey's post hoc test. **P<0.01, ***P<0.001. NC, negative control; miR, microRNA; NS, not significant; AV, Annexin V; PI, propidium iodide.

post hoc test. P<0.05 was considered to indicate a statistically significant difference.

Results

Cell viability and miR-126 expression in the OGD/R model. Cell viability was reduced in the Model group compared with the NC group (P<0.01), suggesting that the construction of the OGD/R model was successful (Fig. 1A). After the establishment of the OGD/R model, RT-qPCR was performed to detect miR-126 expression. The results indicated that miR-126 expression levels were downregulated in the Model group compared with the NC group (P<0.01; Fig. 1B).

miR-126 regulates cell viability and apoptosis during cerebral I/R injury. After transfection with the mimic-miR, miR-126 expression increased compared with the mimic-NC group (P<0.001). There was no difference in miR-126 expression between the Model and the mimic-NC groups (P>0.05; Fig. 2A). These data demonstrated successful transfection.

AV/PI assays demonstrated that apoptosis was significantly reduced in the mimic-miR group compared with the mimic-NC group (P<0.001). There was no difference in apoptosis between the Model and the mimic-NC groups (P>0.05; Fig. 2B and C). Moreover, cell viability was significantly increased in the mimic-miR group compared with the mimic-NC group (P<0.01), but remained similar between the Model and the mimic-NC groups (P>0.05; Fig. 2D).

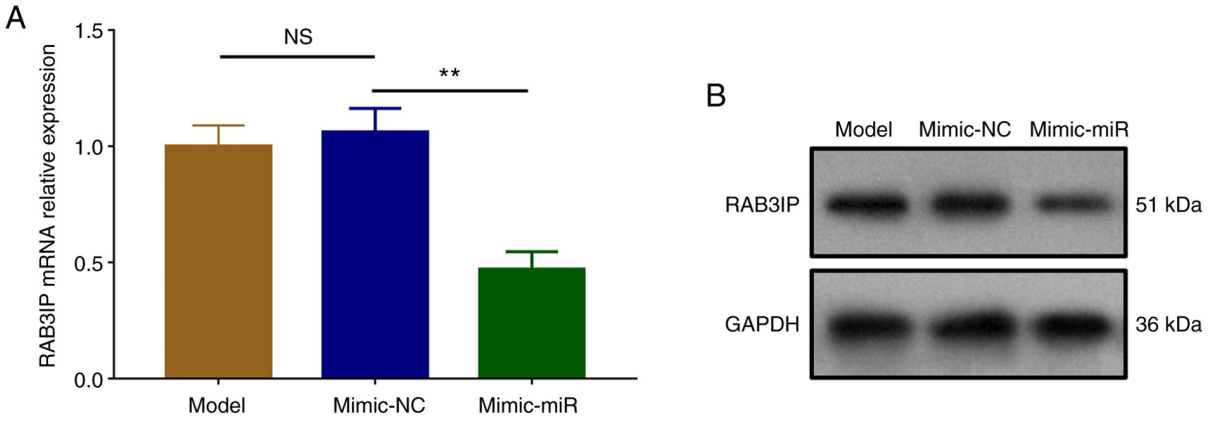

Figure 3. Effect of miR-126 on RAB3IP expression during cerebral ischemia/reperfusion injury. RAB3IP (A) mRNA and (B) protein expression levels were determined using reverse transcription-quantitative PCR and western blotting, respectively. n=3. The data were analyzed using one-way ANOVA followed by Tukey's post hoc test. **P<0.01. NC, negative control; NS, not significant; RAB3IP, Ras-related protein RAB3A interacting protein; miR, microRNA.

Additionally, Hoechst/PI assays confirmed that apoptosis was reduced following mimic-miR transfection (P<0.01), but was similar in the Model and mimic-NC groups (P>0.05; Fig. 2E and F).

miR-126 downregulates RAB3IP expression during cerebral I/R injury. The mRNA (P<0.01) and protein expression levels of RAB3IP were downregulated in the mimic-miR group compared with the mimic-NC group, but similar between the Model and the mimic-NC groups (P>0.05; Fig. 3A and B).

Expression of RAB3IP following transfection. Following transfection, RAB3IP expression increased in the OE-RAB3IP group compared with the OE-NC group (P<0.001). No difference in RAB3IP expression was observed between the Model and the OE-NC groups (P>0.05; Fig. S1). These data demonstrated successful transfection.

miR-126 regulates cell viability, apoptosis and cell cycle progression during cerebral I/R injury via RAB3IP. In order to determine whether miR-126 exerted neuroprotective effects during cerebral I/R injury via RAB3IP, rescue experiments were carried out. The mRNA (P<0.001) and protein expression levels of RAB3IP were upregulated in the OE-RAB3IP + mimic-NC group compared with the OE-NC + mimic-NC group (P<0.001), as well as in the OE-RAB3IP + mimic-miR group compared with the OE-NC + mimic-miR group (P<0.01; Fig. 4A and B). However, there was no difference in miR-126 expression between the OE-RAB3IP + mimic-NC and the OE-NC + mimic-NC groups, nor between the OE-RAB3IP + mimic-miR and the OE-NC + mimic-miR groups (both P>0.05; Fig. 4C).

Cell viability was reduced in the OE-RAB3IP + mimic-NC group compared with the OE-NC + mimic-NC group (P<0.001), as well as in the OE-RAB3IP + mimic-miR group compared with the OE-NC + mimic-miR group (P<0.001; Fig. 4D).

Furthermore, AV/PI assays suggested that apoptosis was significantly increased in the OE-RAB3IP + mimic-NC group compared with the OE-NC + mimic-NC group (P<0.01), as well as in the OE-RAB3IP + mimic-miR group compared with the OE-NC + mimic-miR group (P<0.05; Fig. 4E and F). Hoechst/PI staining also confirmed these findings (Fig. 4G and H).

Cell cycle progression was also analyzed. The number of cells in the G_0/G_1 phase was reduced following mimic-miR transfection compared with the mimic-NC group (P<0.05). By contrast, the number of cells in the S phase increased following transfection with the mimic-miR (P<0.05). However, there was no difference in the number of cells in the G_2 phase (P>0.05; Fig. S2A and B). Moreover, the number of cells in the G_0/G_1 phase was increased in the OE-RAB3IP + mimic-NC group compared with the OE-NC + mimic-NC group (P<0.05), as well as in the OE-RAB3IP + mimic-miR group compared with the OE-NC + mimic-miR group (P<0.05). The number of cells in the S phase was reduced following co-transfection with OE-RAB3IP + mimic-NC compared with the OE-NC + mimic-NC group (P<0.05). This was also the case in the OE-RAB3IP + mimic-miR group compared with the OE-NC + mimic-miR group (P<0.05). There was no difference in the number of cells in the G_2 phase between these groups (all P>0.05; Fig. S2C and D).

Moreover, LDH assays were also carried out, and the results demonstrated that LDH release was increased in the Model group compared with the NC group, suggesting successful construction of the OGD/R model (P<0.01; Fig. S3A). In addition, LDH release was reduced in the mimic-miR group compared with the mimic-NC group (P<0.01), but similar between the Model and mimic-NC groups (P>0.05; Fig. S3B). Additionally, LDH release was increased following co-transfection with OE-RAB3IP + mimic-NC compared with the OE-NC + mimic-NC group (P<0.01). This was also true for OE-RAB3IP + mimic-miR transfection compared with the OE-NC + mimic-miR group (P<0.01; Fig. S3C).

Luciferase reporter assay. The sequences of RAB3IP-WT, RAB3IP-MT and miR-126 are presented in Fig. 5A. Relative luciferase activity was decreased in the RAB3IP-WT + mimic-miR group compared with the RAB3IP-WT + mimic-NC group (P<0.01). However, there was no difference in the relative luciferase activity between

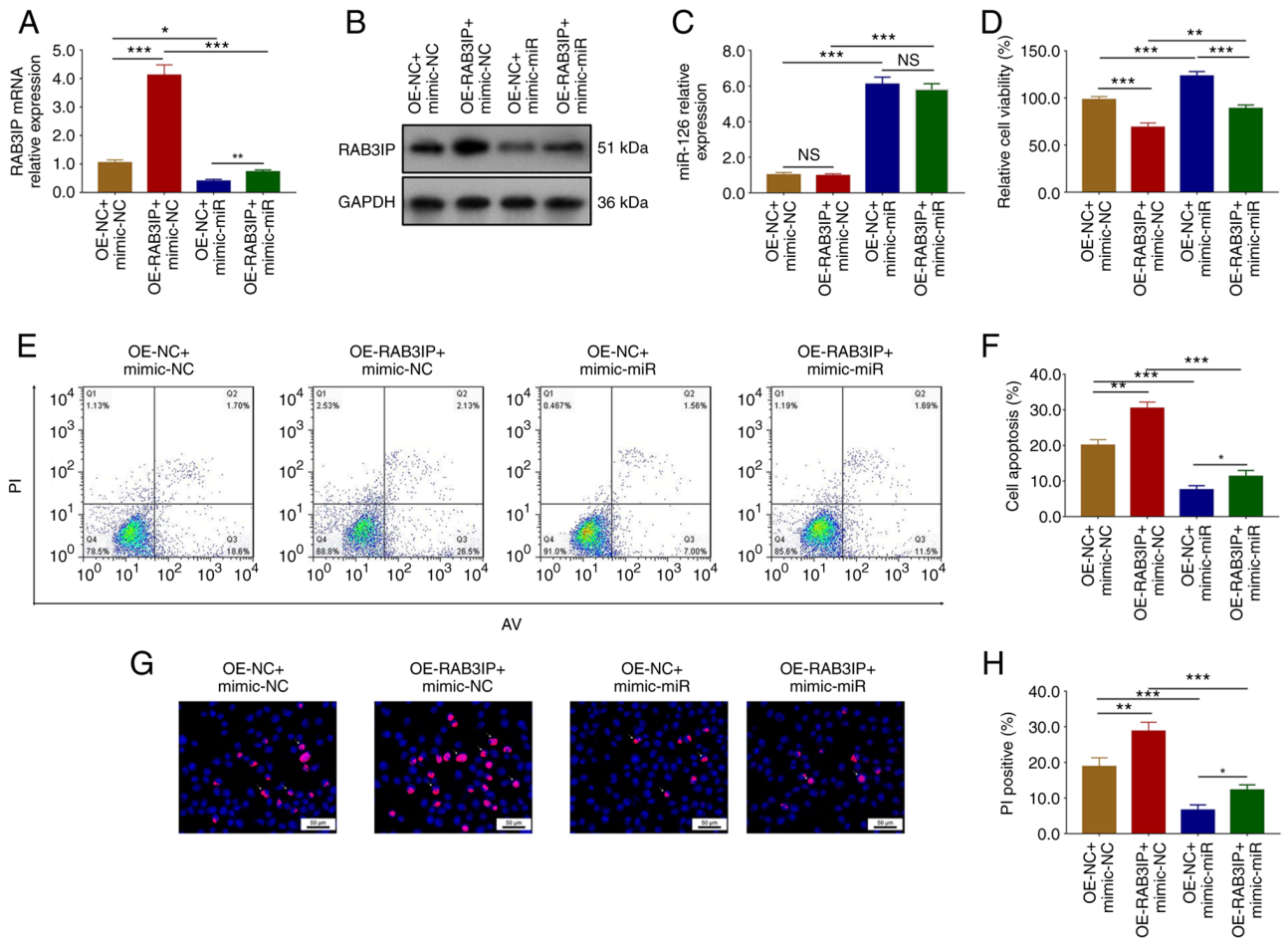

Figure 4. miR-126 regulates cell viability and apoptosis during cerebral ischemia/reperfusion injury via RAB3IP. RAB3IP (A) mRNA and (B) protein expression levels were determined using reverse transcription-quantitative PCR and western blotting, respectively. (C) miR-126 expression levels. (D) Cell viability. (E-H) Apoptosis was determined using AV/PI and Hoechst/PI assays. n=3. The data were analyzed using one-way ANOVA followed by Tukey's post hoc test. *P<0.05, **P<0.01, ***P<0.001. NS, not significant; RAB3IP, Ras-related protein RAB3A interacting protein; miR, microRNA; OE, overexpression; NC, negative control; AV, Annexin V; PI, propidium iodide.

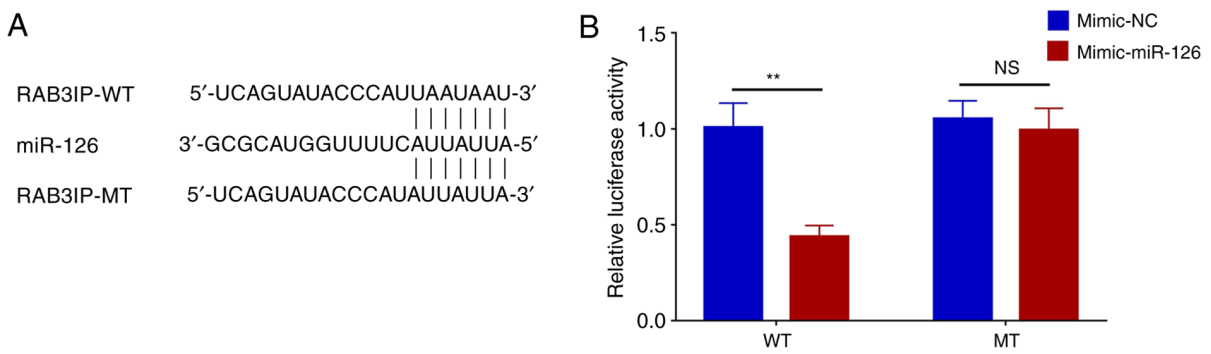

Figure 5. Dual-luciferase reporter assays. (A) Sequences of RAB3IP-WT, -MT and miR-126. (B) Relative luciferase activity in different groups. n=3. The data were analyzed using unpaired Student's t-tests. **P<0.01. NS, not significant; RAB3IP, Ras-related protein RAB3A interacting protein; miR, microRNA; NC, negative control; WT, wild-type; MT, mutant.

RAB3IP-MT + mimic-miR and the RAB3IP-MT + mimic-NC groups (P>0.05; Fig. 5B).

Discussion

To the best of our knowledge, the findings of the present study demonstrated for the first time that miR-126 could reduce the effects of OGD/R in SH-SY5Y cells by targeting RAB3IP. These findings may improve our understanding of the pathogenesis of cerebral I/R injury and provide novel insights into the treatment of this condition.

miR-126 is a well-characterized miRNA that plays a crucial role in a range of pathological processes, including several inflammatory diseases. For example, this miRNA interacts

with the Akt/Rac family small GTPase 1 signaling pathway to inhibit inflammatory responses during sepsis (16). Moreover, miR-126 inhibits stromal cell-derived factor-1 (SDF-1) α and C-C motif chemokine ligand 2 expression to inhibit the recruitment of inflammatory monocytes into the tumor stroma, thereby suppressing breast cancer metastasis (17). Furthermore, miR-126 targets TNF receptor associated factor 6 to reduce the expression of pro-inflammatory cytokines in human gingival fibroblasts under high-glucose conditions (28). In addition to its inhibitory function in various inflammatory diseases, miR-126 also serves a role in neuroregulation in several nervous system diseases. For example, miR-126 targets RAB3IP to increase 1-methyl-4-phenylpyridine-induced SH-SY5Y neuronal cell proliferation and reduce apoptosis in a model of Parkinson's disease (18). In addition, miR-126 regulates the SDF-1/C-X-C chemokine receptor (CXCR)7 pathway to promote post-stroke angiogenesis of endothelial progenitor cell transplantation (29).

Furthermore, miR-126 has emerged as a critical regulatory molecule during I/R injury. For example, hematopoietic miR-126 is related to stromal cell-derived factor 1/CXCR4-dependent vasculogenic progenitor cell mobilization to promote vascular integrity, thereby protecting against renal I/R injury (30). In addition, miR-126 promotes Nrf2 expression to reduce oxidative stress and renal I/R injury (19). miR-126 also decreases oxidative stress and apoptosis from myocardial I/R injury by targeting epidermal growth factor receptor feedback inhibitor 1 (20). Despite the protective effect of miR-126 against I/R injury in several organs, limited evidence is available regarding its role during cerebral I/R injury. As miR-126 can inhibit inflammation in neuronal cells, it was hypothesized that miR-126 may exert a protective role in cerebral I/R injury. In the present study, an OGD/R model was established in order to simulate cerebral I/R injury *in vitro*. miR-126 expression was downregulated in the OGD/R model. It is possible that miR-16 binds to several genes to decrease oxidative stress and reduce miR-126 expression. In order to further explore the effect of miR-126 on cell viability and apoptosis during cerebral I/R injury, miR-126 mimic transfection was carried out in SH-SY5Y cells, which were then subjected to OGD/R treatment. The results demonstrated that miR-126 could promote cell viability during OGD/R, whilst inhibiting apoptosis. This suggested that miR-126 could protect SH-SY5Y cells in this model of I/R injury. The probable explanations were that: i) miR-126 could interact with multiple genes and pathways to promote cell viability and suppress apoptosis (19,31); ii) miR-126 increased cell viability following OGD/R, but decreased apoptosis by targeting several genes (including RAB31P), which subsequently contributed to its the inhibitory effect on I/R injury; and iii) miR-126 regulated several genes and interacted with multiple signaling pathways to inhibit the inflammatory response, thereby decreasing inflammatory-induced neuronal injury and exerting neuroprotective effects during cerebral I/R injury (16,17).

RAB3IP, also known as Rabin 8, is a Rab-specific guanine nucleotide exchange factor (GEF) and a major activator of Rab proteins, which is directly regulated by Rab11 and is involved in multiple biological processes, including neuronal development (32). For example, a previous study suggested that RAB3IP regulates nerve growth factor-induced neurite outgrowth by interacting with Rab8, Rab10, Rab11 or through a GEF-independent mechanism (33). Another study demonstrated that RAB3IP was predominantly enriched in the Golgi apparatus in soma and proximal dendrites, where it regulates Rab8 function to form and/or deliver post-Golgi vesicles to the dendritic membrane, thereby promoting synapse development and increasing spine head diameter (34). In addition, RAB3IP inhibits cell proliferation, but promotes apoptosis in Parkinson's disease (21). Considering the important role of RAB3IP in neuronal development, it was hypothesized in the present study that miR-126 targeted RAB3IP to exert beneficial effects on neuronal cells during cerebral I/R injury.

In order to validate this hypothesis, rescue experiments were performed, which revealed that miR-126 attenuated the OGD/R-induced cell apoptosis, possibly via RAB3IP. Moreover, in a dual-luciferase reporter assay, miR-126 was shown to interact with RAB3IP. Thus, miR-126 might regulate the protein expression of RAB3IP by directly binding to RAB3IP mRNA, thereby regulating cell viability, apoptosis and cell cycle progression in the present cerebral I/R injury model (Fig. S4). Although the present study focused on exploring the underlying mechanism of miR-126/RAB3IP modulation of cellular function after cerebral I/R injury, additional *in vivo* experiments are needed to validate the findings. When detecting cell viability using CCK-8 and MTT assays, cell proliferation may affect the accuracy of the results of cell viability. However, an LDH assay was used to overcome this limitation.

In conclusion, miR-126 protected against I/R-induced cerebral injury by targeting RAB3IP. These findings offer a novel perspective for the underlying mechanism of cerebral I/R injury and may provide valuable insight for the development of potential prevention strategies against cerebral I/R injury.

Acknowledgements

Not applicable.

Funding

No funding was received.

Availability of data and materials

The datasets used and/or analyzed during the current study are available from the corresponding author on reasonable request.

Authors' contributions

ZS and XZ designed the experiments. MZ and JL performed the experiments and acquired the data. NL, YZ, CC, YG and QF analyzed the data. ZS and XZ confirm the authenticity of all the raw data. All authors wrote the manuscript and revised the manuscript. All authors have read and approved the final manuscript.

Ethics approval and consent to participate

Not applicable.

Patient consent for publication

Not applicable.

Competing interests

The authors declare that they have no competing interests.

References

1. Kalogeris T, Baines CP, Krenz M and Korthuis RJ: Ischemia/Reperfusion. Compr Physiol 7: 113-170, 2016.
2. Sakai S and Shichita T: Inflammation and neural repair after ischemic brain injury. Neurochem Int 130: 104316, 2019.
3. Jacob B, Stock D, Chan V, Colantonio A and Cullen N: Predictors of in-hospital mortality following hypoxic-ischemic brain injury: A population-based study. Brain Inj 34: 178-186, 2020.
4. Galkin A: Brain ischemia/reperfusion injury and mitochondrial complex I damage. Biochemistry (Mosc) 84: 1411-1423, 2019.
5. Eltzschig HK and Eckle T: Ischemia and reperfusion-from mechanism to translation. Nat Med 17: 1391-1401, 2011.
6. Kleindorfer DO, Towfighi A, Chaturvedi S, Cockroft KM, Gutierrez J, Lombardi-Hill D, Kamel H, Kernan WN, Kittner SJ, Leira EC, *et al*: 2021 Guideline for the prevention of stroke in patients with stroke and transient ischemic attack: A guideline from the American heart association/American stroke association. Stroke 52: e364-e467, 2021.
7. Gladstone DJ, Lindsay MP, Douketis J, Smith EE, Dowlatshahi D, Wein T, Bourgoin A, Cox J, Falconer JB, Graham BR, *et al*: Canadian stroke best practice recommendations: Secondary prevention of stroke update 2020. Can J Neurol Sci: Jun 18, 2021 (Epub ahead of print).
8. Pantazi E, Bejaoui M, Folch-Puy E, Adam R and Rosello-Catafau J: Advances in treatment strategies for ischemia reperfusion injury. Expert Opin Pharmacother 17: 169-179, 2016.
9. Ibanez B, Heusch G, Ovize M and Van de Werf F: Evolving therapies for myocardial ischemia/reperfusion injury. J Am Coll Cardiol 65: 1454-1471, 2015.
10. Hausenloy DJ and Yellon DM: Myocardial ischemia-reperfusion injury: A neglected therapeutic target. J Clin Invest 123: 92-100, 2013.
11. Zuo ML, Wang AP, Song GL and Yang ZB: MiR-652 protects rats from cerebral ischemia/reperfusion oxidative stress injury by directly targeting NOX2. Biomed Pharmacother 124: 109860, 2020.
12. Xie YL, Zhang B and Jing L: MiR-125b blocks Bax/Cytochrome C/Caspase-3 apoptotic signaling pathway in rat models of cerebral ischemia-reperfusion injury by targeting p53. Neurol Res 40: 828-837, 2018.
13. Di Y, Lei Y, Yu F, Changfeng F, Song W and Xuming M: MicroRNAs expression and function in cerebral ischemia reperfusion injury. J Mol Neurosci 53: 242-250, 2014.
14. Yu Y, Du L and Zhang J: Febrile seizure-related miR-148a-3p exerts neuroprotection by promoting the proliferation of hippocampal neurons in children with temporal lobe epilepsy. Dev Neurosci 43: 312-320, 2021.
15. Liu R, Peng Z, Zhang Y, Li R and Wang Y: Upregulation of miR128 inhibits neuronal cell apoptosis following spinal cord injury via FasL downregulation by repressing ULK1. Mol Med Rep 24: 667, 2021.
16. Wang HF, Wang YQ, Dou L, Gao HM, Wang B, Luo N and Li Y: Influences of up-regulation of miR-126 on septic inflammation and prognosis through AKT/Rac1 signaling pathway. Eur Rev Med Pharmacol Sci 23: 2132-2138, 2019.
17. Zhang Y, Yang P, Sun T, Li D, Xu X, Rui Y, Li C, Chong M, Ibrahim T, Mercatali L, *et al*: MiR-126 and miR-126* repress recruitment of mesenchymal stem cells and inflammatory monocytes to inhibit breast cancer metastasis. Nat Cell Biol 15: 284-294, 2013.
18. Lin Q, Hou S, Dai Y, Jiang N and Lin Y: LncRNA HOTAIR targets miR-126-5p to promote the progression of Parkinson's disease through RAB3IP. Biol Chem 400: 1217-1228, 2019.
19. Zhao B, Chen X and Li H: Protective effects of miR-126 specifically regulates Nrf2 through ischemic postconditioning on renal ischemia/reperfusion injury in mice. Transplant Proc 52: 392-397, 2020.
20. Wang W, Zheng Y, Wang M, Yan M, Jiang J and Li Z: Exosomes derived miR-126 attenuates oxidative stress and apoptosis from ischemia and reperfusion injury by targeting ERRFI1. Gene 690: 75-80, 2019.
21. Zhang JF, Shi LL, Zhang L, Zhao ZH, Liang F, Xu X, Zhao LY, Yang PB, Zhang JS and Tian YF: MicroRNA-25 negatively regulates cerebral ischemia/reperfusion injury-induced cell apoptosis through Fas/FasL pathway. J Mol Neurosci 58: 507-516, 2016.
22. Wang Y and Xu M: MiR-380-5p facilitates NRF2 and attenuates cerebral ischemia/reperfusion injury-induced neuronal cell death by directly targeting BACH1. Transl Neurosci 12: 210-217, 2021.
23. Yu G, Sun W, Wang W, Le C, Liang D and Shuai L: Overexpression of microRNA-202-3p in bone marrow mesenchymal stem cells improves cerebral ischemia-reperfusion injury by promoting angiogenesis and inhibiting inflammation. Aging (Albany NY) 13: 11877-11888, 2021.
24. Shi Y, Yi Z, Zhao P, Xu Y and Pan P: MicroRNA-532-5p protects against cerebral ischemia-reperfusion injury by directly targeting CXCL1. Aging (Albany NY) 13: 11528-11541, 2021.
25. Livak KJ and Schmittgen TD: Analysis of relative gene expression data using real-time quantitative PCR and the 2(-Delta Delta C(T)) Method. Methods 25: 402-408, 2001.
26. Chen C, Ridzon DA, Broomer AJ, Zhou Z, Lee DH, Nguyen JT, Barbisin M, Xu NL, Mahuvakar VR, Andersen MR, *et al*: Real-time quantification of microRNAs by stem-loop RT-PCR. Nucleic Acids Res 33: e179, 2005.
27. Kramer MF: Stem-loop RT-qPCR for miRNAs. Curr Protoc Mol Biol Chapter 15: Unit 15 10, 2011.
28. Wu Y, Song LT, Li JS, Zhu DW, Jiang SY and Deng JY: MicroRNA-126 regulates inflammatory cytokine secretion in human gingival fibroblasts under high glucose via targeting tumor necrosis factor receptor associated factor 6. J Periodontol 88: e179-e187, 2017.
29. Shan C and Ma Y: MicroRNA-126/stromal cell-derived factor 1/C-X-C chemokine receptor type 7 signaling pathway promotes post-stroke angiogenesis of endothelial progenitor cell transplantation. Mol Med Rep 17: 5300-5305, 2018.
30. Bijkerk R, van Solingen C, de Boer HC, van der Pol P, Khairoun M, de Bruin RG, van Oeveren-Rietdijk AM, Lievers E, Schlagwein N, van Gijlswijk DJ, *et al*: Hematopoietic microRNA-126 protects against renal ischemia/reperfusion injury by promoting vascular integrity. J Am Soc Nephrol 25: 1710-1722, 2014.
31. Xiao ZH, Wang L, Gan P, He J, Yan BC and Ding LD: Dynamic Changes in miR-126 expression in the hippocampus and penumbra following experimental transient global and focal cerebral ischemia-reperfusion. Neurochem Res 45: 1107-1119, 2020.
32. Ren H, Xu Z, Guo W, Deng Z and Yu X: Rab3IP interacts with SSX2 and enhances the invasiveness of gastric cancer cells. Biochem Biophys Res Commun 503: 2563-2568, 2018.
33. Homma Y and Fukuda M: Rabin8 regulates neurite outgrowth in both GEF activity-dependent and -independent manners. Mol Biol Cell 27: 2107-2118, 2016.
34. Ultanir SK, Hertz NT, Li G, Ge WP, Burlingame AL, Pleasure SJ, Shokat KM, Jan LY and Jan YN: Chemical genetic identification of NDR1/2 kinase substrates AAK1 and Rabin8 Uncovers their roles in dendrite arborization and spine development. Neuron 73: 1127-1142, 2012.